ACS APPLIED BIO MATERIALS Cite This: ACS Appl. Bio Mater. 2020, 3, 197−207 Article www.acsabm.org

Silica Release from Silane Cross-Linked Gelatin Based Hybrid Scaffold Affects Cell Proliferation

Chelladurai Karthikeyan Balavigneswaran,[†,∥] Ramya Venkatesan,[⊥] Prakash Shyam Karuppiah,[#] Gaurav Kumar,[§] Pankaj Paliwal,[‡] Sairam Krishnamurthy,[‡] Balamuthu Kadalmani,[⊥] Sanjeev Kumar Mahto,[‡] and Nira Misra*[,†]

[†]Polymer Engineering Laboratory and [‡]Tissue Engineering and Biomicrofluidics Laboratory, [§]Electrophysiology Lab, School of Biomedical Engineering, and Indian Institute of Technology (Banaras Hindu University), Varanasi-221005, Uttar Pradesh, India

[∥]Tissue Engineering and Biomaterials Lab, Department of Biotechnology, Bhupat and Jyoti Mehta School of Biosciences, Indian Institute of Technology Madras, Chennai-600036, Tamil Nadu, India

[#]Research and Development Division, VVD and Sons Private Limited, Thoothukudi-621004, Tamil Nadu, India

[⊥]Department of Animal Science, Bharathidasan University, Tiruchirappalli-620024, Tamil Nadu, India

Supporting Information

ABSTRACT: Earlier, we had reported the synthesis and characterization of star-shaped poly(D,L-lactide)-*b*-gelatin (ss-pLG) to improve cell adhesion and proliferation, but the stability of ss-pLG scaffolds remained a persistent issue. Here we show an increase in the stability of ss-pLG using 3-glycidoxypropyl trimethoxysilane (GPTMS) as a covalent cross-linker (h-ss-pLG). The rate of cell proliferation within Hep-G2 cultured h-ss-pLG scaffolds increased until the third day, and afterward it drastically declined. Further, we identified the release of inorganic silica from GPTMS cross-linked h-ss-pLG, which may be associated with the decrease in the rate of HepG2 cell proliferation. However, the cross-linking did not affect red blood cells (RBCs) and they were completely hemocompatible. In addition, our *in vivo* experiments in female rats showed that the hybrid h-ss-pLG scaffolds were not degraded completely after 4 weeks, as they were covalently cross-linked with silane. These results suggest the significance of the cross-linker selection, which is one of the other key factors, and needs to be considered while designing scaffolds.

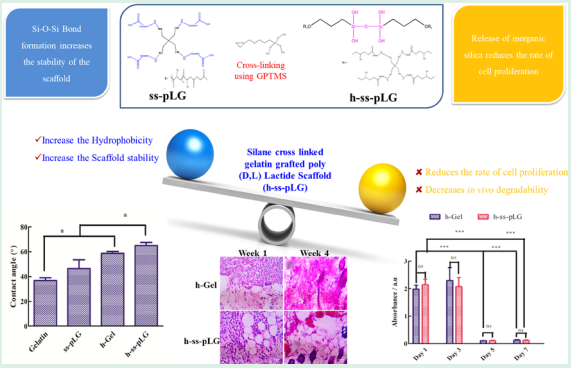

KEYWORDS: *Polylactic acid (PLA), gelatin, glycidoxypropyl trimethoxysilane (GPTMS), cross-linking, cell proliferation*

1. INTRODUCTION

Biomaterials based tissue engineering is a popular approach to solve the problem of degeneration of tissue; however, suitable biomaterials must meet some challenging criteria.[1] For example, the template for the tissue growth which is mentioned as the scaffold should exhibit better stability to match the mechanical properties of the host tissue, and resorb with a tailored degradation rate. Poly(lactic acid) (PLA) has received momentous attention and is considered to be the most promising biopolymer for tissue engineering applications owing to its biodegradable nature. The stability, degradation rate, and mechanical strength of PLA-based 3D scaffolds can be increased by hydroxyapatite,[2] bioactive glass,[3] and cacium phosphate.[4] On the other hand, gelatin is a commercially available natural protein that is widely used as a tissue engineering scaffold due to its biodegradability and similarity to the more expensive collagen adhesive protein. To increase the stability of the gelatin based scaffolds, people have used various cross-linkers such as glutaraldehyde,[5,6] EDC·HCl,[7,8] and genipin.[9] However, the use of those cross-linkers are limited because of their potential toxic effects and ineffective increase in mechanical strength. In addition, sol−gel derived hybrid materials have also been used, where interpenetrating networks (IPNs) of organic polymers and inorganic components form biodegradable composite scaffolds.[10−13] Among the inorganic components, silica-based bioactive glasses are an important class of materials because of the tailored chemical property and controlled degradation when cross-linked with polymers.[3,14]

Earlier, we had reported tailored chemical properties of 4-arm star-shaped poly(D,L-lactide) as cell-adhesive three-dimensional scaffolds.[15] We circumvented the problem of the lack of cell adhering functional moieties in PLA by grafting gelatin to star-shaped (4 arms) poly(D,L-lactide) (ss-PDLLA). The gelatin grafted star-shaped poly(D,L-lactide)-*b*-gelatin (ss-pLG) exhibited lower contact angle, i.e., the hydrophilicity

Received: July 29, 2019
Accepted: December 8, 2019
Published: December 9, 2019

DOI: 10.1021/acsabm.9b00680
ACS Appl. Bio Mater. 2020, 3, 197−207

was increased. However, we observed that scaffolds fabricated from ss-pLG degraded at a faster rate because of the gelatin grafting. Further, we developed linear PDLLA-*b*-gelatin (l-pLG)[16] that somehow controlled the degradation rate because of the degree of gelatin grafting, but the stability of the scaffolds was not that much higher to support cells for a longer period. On the other hand, the biocompatible silica possesses very good cell adhesion property.[17−19] To increase the stability of the ss-pLG scaffolds, we introduced the cross-linker based upon the following rationale: The silica alone is brittle; further, if polymers are introduced to the silica, the resulting hybrid composites with silica will potentially increase the stability and toughness of the materials, which could be particularly useful for tissue engineering applications. In that view, γ-glycidoxypropyltrimethoxysilane (GPTMS) was taken as a cross-linker, which is a known silane coupling agent that consists of epoxy and methoxysilane groups. The epoxy ring of the GPTMS molecules react with the amino or carboxyl groups on the polymeric chain and forms pendent silanol groups (Si−OH) by hydration of the trimethoxy groups on the GPTMS via an acid-catalyzed reaction. Further, the condensation process of two Si−OH molecules allows the formation of Si−O−Si bonds. Thus, the cross-linked structures form through Si−O−Si linkages.[20−25]

In the present study, cross-linking of ss-pLG with GPTMS (h-ss-pLG) and their cellular proliferation on the hybrid scaffold is demonstrated. The covalent cross-linking will increase the hydrophobicity and thus the stability of the matrix. In accordance with our hypothesis, we studied the contact angle and validated the newly synthesized h-ss-pLG for their biocompatibility and biodegradability by *in vitro* culturing of hepatocyte (Hep-G2) cells within the h-ss-pLG scaffolds and *in vivo* subcutaneous implantation of the h-ss-pLG in female rats. On the other hand, we also prepared gelatin cross-linked scaffolds (h-Gel) for the comparative study.

2. MATERIALS AND METHODS

2.1. Chemicals and Materials. 3,6-Dimethyl-1,4-dioxane-2,5-dione (D,L-lactide), Tin(II) 2-ethylhexanoate, *N*-hydroxusuccinimide (NHS), (3-Glycidyloxypropyl)trimethoxysilane (GPTMS), Hematoxylin-Eosin (H&E) solution, and methylthiazolyldiphenyl-tetrazolium bromide salt (MTT) were purchased from Sigma-Aldrich. Pentaerythritol was procured from SRL chem. lab. Dialysis tubing having MWCO = 100 000 was purchased from Cole Parmer. Analytical grade solvents like dichloromethane (DCM), tetrahydrofuran (THF), dimethyl sulfoxide (DMSO), dimethylformamide (DMF), and hydrochloric acid (HCl) were purchased from SRL chem. lab. Other materials and chemicals were purchased from Hi-media unless specified in the text.

2.2. Synthesis of Hybrid Star-Shaped Poly(D,L-Lactide) Grafted Gelatin (h-ss-pLG). Synthesis of ss-pLG was done according to our previously reported paper.[15] Further, 10% of ss-pLG was prepared in DMSO and water containing 10 mM hydrochloric acid (HCl) (300 μL in 3 mL). Then, GPTMS was added in equal molar ratio (the mole ratio of GPTMS/gelatin; molecular weight of gelatin was considered as 90 000 g/mol) and stirred overnight at temperature 70 °C. Equimolar ratio was chosen based on the optimization experiments carried out (data not shown); the disappearance of Si−OH band at 910 cm^{-1} and the appearance of a broadened Si−O−Si band at 1115 cm^{-1} in the FT-IR spectrum were considered as successful cross-linking. The hybrid gelatin (h-Gel) was also prepared in the same way as h-ss-pLG was prepared. After 12 h of reaction, the hybrid gels were dialyzed against water for 48 h.

2.3. Characterization of Polymer. *2.3.1. FTIR Study.* FTIR was done using PerkinElmer IR spectrophotometer (PerkinElmer Inc., USA) in ATR mode.[15,16]

2.3.2. Thermogravimetric Analysis (TGA). Mettler TGA thermogravimetric analyzer was used to characterize thermal properties of polymers. Temperature ranging from 40 to 800 °C was analyzed with a heating rate of 20 °C/min under N_2 atmosphere.

2.3.3. Differential Scanning Calorimetry (DSC) Analysis. DSC was carried out using Mettler STAR SW 10.00 instrument under nitrogen atmosphere. The samples were first heated until 150 °C at 10 °C min^{-1} heating rate and then quenched to −50 °C to remove the moisture or water present in the sample. The second heating run from 37 to 200 °C was performed. Results were reported from the second heating run.

2.3.4. Water Contact Angle Measurement. Water contact angle was measured with a Kruss K100 tensiometer and the associated software using our previously reported protocol.[15,26]

2.4. Fabrication of 3D Unmodified and Hybrid Scaffolds. Scaffolds were fabricated by freeze−drying technique.[27] Briefly, 10% hybrid gel was prepared. 50 μL polymer solution was poured onto the wells of a 96 well plate and cured at 70 °C for overnight. Further, the cured gel was kept at −20 °C overnight. Thereafter, the gels were held at −80 °C for 4 days using a freeze−dryer (LyoQuest 85, Telstar, Spain). The scaffolds were stored in a vacuum desiccator until further use.

2.5. Characterization of Scaffolds by Scanning Electron Microscopy (SEM). Surface morphology of scaffolds was evaluated by Scanning Electron Microscopy (Zeiss Evo18, Germany). ImageJ software was used to calculate the pore sizes from SEM images.

The morphology of hepatocytes (Hep-G2) was also evaluated using SEM. After 3 days culturing of cells within hybrid scaffolds, they were taken out from cell culture media and washed with PBS three times. Further, they were fixed with 4% paraformaldehyde (PFA) for 15 min. The cell-fixed scaffolds were again washed with PBS to remove PFA and stored at 4 °C with PBS until the characterization. Before the characterization, scaffolds were treated with a series of ethanol treatments such as 50%, 60%, 70%, 90%, and 100% ethanol. The dried scaffolds were gold sputtered and imaged under SEM (Zeiss Evo18, Germany).

The hybrid scaffolds (h-Gel and h-ss-pLG) incubated in red blood cells (RBCs) were taken out from the shaking incubator after 4 h. They were washed with PBS 3 times. Then, RBCs were fixed with 1% glutaraldehyde for 15 min, and washed 3 times. The fixed RBCs were stored in 4 °C until the further characterization. The blood smear was gold sputtered and imaging was done using scanning electron microscopy (Zeiss Evo18, Germany).

2.6. Silica Release Profile. The silica release profile from the hybrid scaffolds was analyzed in cell culture media. The scaffolds having the dimensions of 8 mm diameter were put into 200 μL DMEM/FBS containing cell culture media. After days 1, 3, 5, and 7, the scaffolds were washed with PBS. Further, the scaffolds were analyzed by FTIR and energy-dispersive X-ray spectroscopy along with elemental mapping. All the experiments were done in triplicate.

2.7. Cell Culture. Hepatocytes Hep-G2 was procured from NCCS, Pune, India. Cells were cultured in Dulbecco's modified eagle's medium (DMEM) (high glucose), with 10% fetal bovine serum (FBS) and 1% penicillin streptomycin in a CO_2 incubator at 37 °C with 5% CO_2, 95% humidity. During the culture, medium was changed every 2 days. For the cell culturing on 3D scaffolds, scaffolds were initially kept in 100% ethanol for 30 min and then sterilized under UV for 30 min. Then, the scaffolds were soaked in cell culture media and kept in CO_2 incubator at 37 °C for 30 min. Cells were counted and concentrated into volume of 20−25 μL; further, they were seeded into the scaffolds and kept in a CO_2 incubator for 3 h to allow the cells to attach and settle into the scaffolds. After 3 h of incubation, fresh media was added.

2.7.1. Cell Viability and Proliferation. The fabricated scaffolds were studied for cell viability using MTT assay.[15,28] Cell numbers were normalized to 1 according to the observation of cell growth in 2D culture plate on the third day.

DOI: 10.1021/acsabm.9b00680
ACS Appl. Bio Mater. 2020, 3, 197−207

Scheme 1. Reaction Scheme for the Synthesis of Silane Cross-Linked Gelatin Grafted Star-Shaped PDLLA (h-ss-pLG)

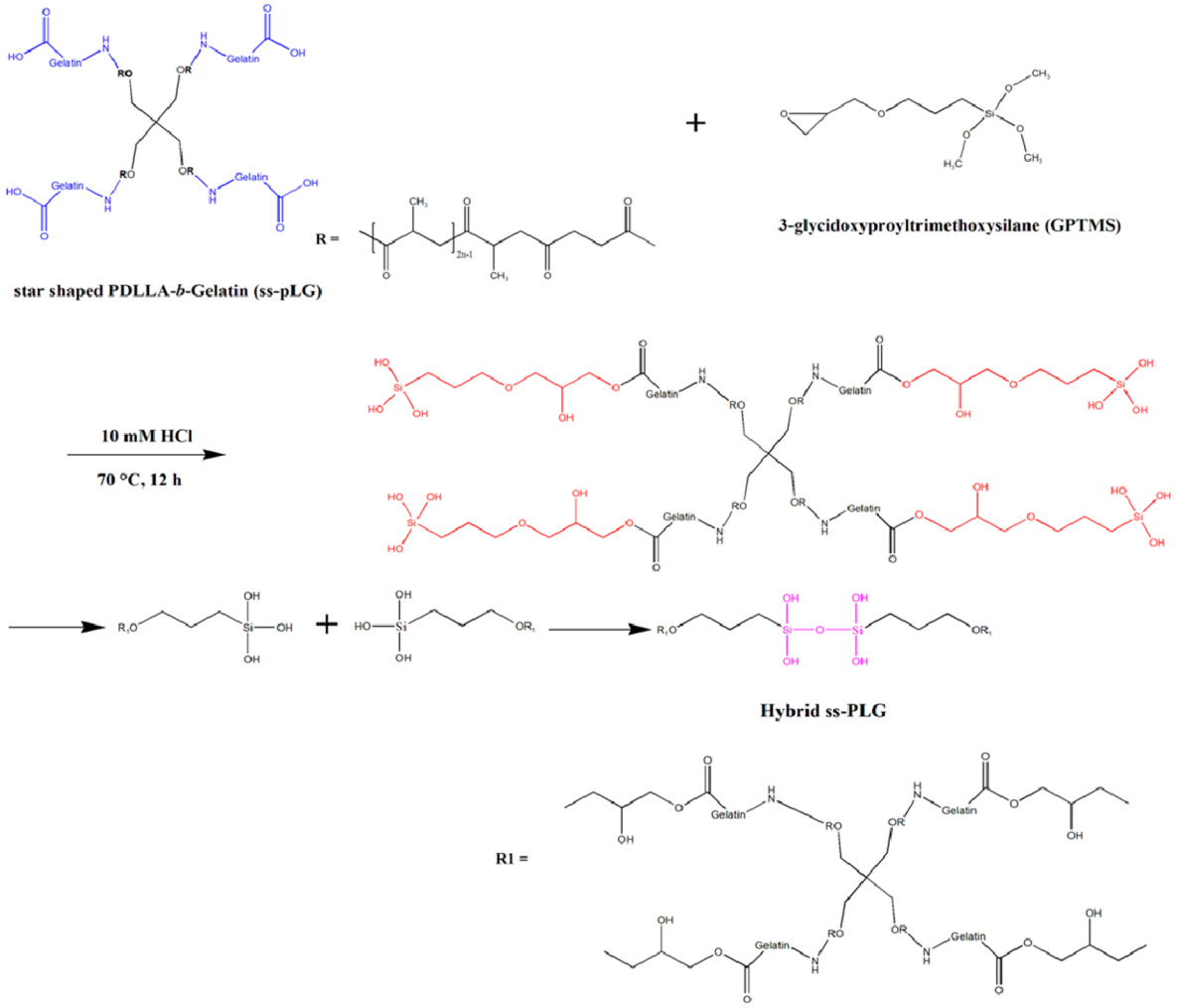

For the GPTMS cytotoxicity, various concentrations (0.1%, 0.2%, 0.5%, 1.0%, and 2.0%) were prepared in DMSO and 20 μL sample was added to the growing cell. After 3 day of culturing, MTT was added and cytotoxicity of GPTMS was found. All the experiments were done in triplicate.

2.7.2. Molecular Gene Expression Study by Quantitative-Reverse-Transcription PCR (qPCR). 2.7.2.1. RNA Isolation. RNA was isolated from cultured HepG2 cells grown in scaffolds after 1/5/7 days using TRIzol reagent (Thermo Fisher, USA) as per manufacturer's recommendation. All steps were performed at room temperature (20−25 °C). The RNA thus obtained was stored at −80 °C until further use. The RNA yield was calculated by diluting the sample in RNase-free water and measuring the absorbance at 260 and 280 nm. We calculated the RNA concentration using the formula

$$\text{A260} \times \text{dilution} \times 40 = x\ \mu\text{gRNA/mL}$$

The purity of the RNA was calculated by obtaining the A260/A280 ratio. A ratio of ∼2 was considered pure.

2.7.2.2. cDNA Synthesis. The cDNA was synthesized using the previously reported protocols.[29] The samples were first treated with 2 U/μL DNase to remove all traces of genomic DNA. The Primer 3 software was used to design SYBR Green oligonucleotide primers for the real-time quantitative PCR (qRT-PCR) experiment for analyzing β-actin, TWIST, SOX2, and VEGF. Human β-actin expression was used as an in-house control. cDNA was synthesized using a cDNA-reverse-transcription kit (TaKaRa Bio.Inc., Tokyo) as per the manufacturer's instructions.

2.7.2.3. Quantitative Real-Time PCR. Quantitative real-time PCR (qRT-PCR) was carried out using a LightCycler 96 System (Roche Molecular Systems, Inc., India) with cDNA as the template at following conditions: PCR − 42 cycles, preincubation at 95 °C for 5 min, denaturation at 95 °C for 10 s, annealing at 60 °C for 10 s, and elongation at 72 °C for 10 s. Gene expression was normalized to β-actin.

2.7.2.4. Calculation of Fold Change ($2^{-\Delta\Delta cq}$). Fold change was calculated using the $2^{-\Delta\Delta cq}$ method.[30] Briefly, triplicate expression values were calculated and averaged for individual time points. Gene of interest (TWIST, SOX2, VEGF) were designated as test expression (Cq^{TE}) whereas the average expression values for housekeeping genes were designated as housekeeping expression (Cq^{HE}). ΔCq is the difference in threshold cycle between the target and reference genes. ΔCq for sample A (h-Gel) was calculated as follows: $\Delta Cq^{A} = Cq^{TE} - Cq^{HE}$. Similarly ΔCq for sample B (ΔCq^{B}) (h-ss-pLG) and control (cells cultured in 96 well plate) (ΔCq^{H}) were calculated, individually. ΔΔCq for h-Gel ($\Delta\Delta Cq^{A}$) was calculated by subtracting ΔCq^{H} from ΔCq^{A}. Similarly, $\Delta\Delta Cq^{B}$ for h-ss-pLG was calculated. Finally, the calculated ΔΔCq values were raised to the power 2^{-x}, where x is ΔΔCq.[30] Table S1 shows the sequences of the primers used in the study.

2.8. Hemocompatibility of Scaffolds. *2.8.1. Blood Sample.* Blood samples were collected in a 15 mL centrifuge tube containing EDTA as an anticoagulant, from Blood Bank, Banaras Hindu University (BHU), Varanasi, India.

2.8.2. Hemolysis. The hemolysis of the hybrid scaffolds after 1 and 8 h was studied using the reported papers.[15,31]

2.8.3. Evaluation of Erythrocyte Membrane Integrity. Lactate dehydrogenase (LDH) enzymes released from the erythrocyte incubated hybrid scaffolds were photometrically detected after

DOI: 10.1021/acsabm.9b00680
ACS Appl. Bio Mater. 2020, 3, 197−207

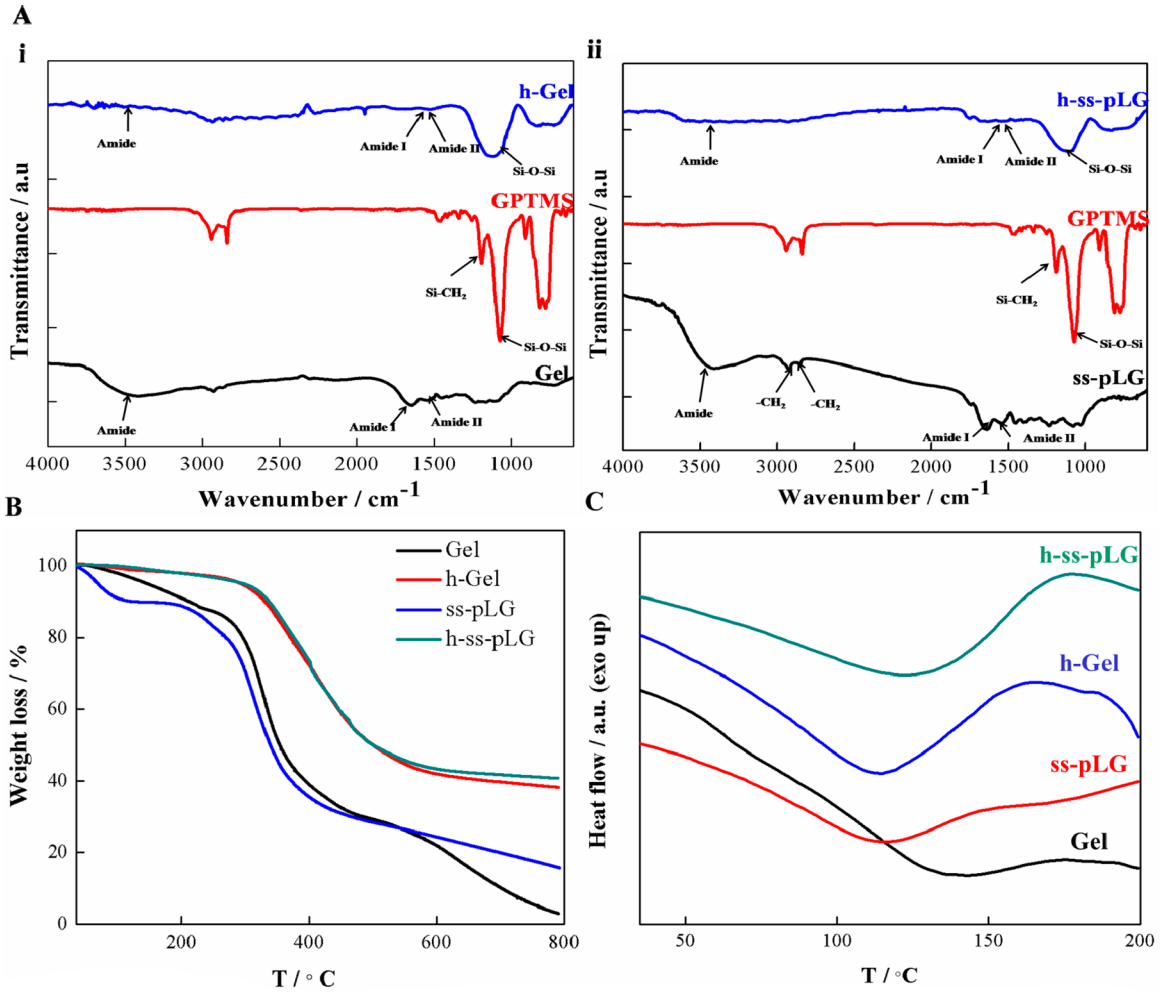

Figure 1. Characterization of hybrid gels. FTIR spectra of (A) silane cross-linked gelatin (h-Gel) and (B) silane cross-linked ss-pLG (h-pLG). Thermal properties of hybrid gels. (B) TGA and (C) DSC thermograms of gelatin-grafted and silane cross-linked hybrid polymers.

treatmsnf with scaffold samples by LDH commercial assay kit (Tulip Diagnostics, India).[32] The previously reported procedures were followed without any modification.[15,31]

2.9. Subcutaneous *in Vivo* Implantation of Scaffolds and Their Immune Response. The animals were acclimatized for 2 weeks in laboratory condition (25 ± 2 °C), with 12 h light/dark cycle. All *in vivo* experiments were conducted as per the guidelines of the Central Animal Ethical Committee, Institute of Medical Sciences, Banaras Hindu University (BHU), Varanasi, India (Registration No. 542/02/ab/CPCSEA). We used female Charles−Foster (CF) rats having the weight of 220−220 g body weight. The rats were subcutaneously implanted with acellular Gel, ss-PDLLA, ss-pLG, and the hybrid h-ss-pLG, h-Gel scaffolds that have the specific dimensions (8 mm in diameter, 2 mm in height). The study was conducted for two time points: week 1 and week 4. The weight loss was observed for the course of the experiment. Moreover, no animal death was observed during the experimental period. After 1 and 4 weeks of implantation, scaffolds were retrieved from the implanted site with the overlying native tissues. The scaffolds with tissues were put into 10% formaldehyde for 48 h and processed, and tissue sections were prepared for histology according to previously reported procedures.[33]

2.10. Statistical Analysis. All measurements were reported as mean ± standard deviation (SD), n = 3 with a confidence level of 95%. GraphPad Prism v 5 was used to test the statistical difference using one-way ANOVA and two-way ANOVA.

3. RESULTS AND DISCUSSION

3.1. Synthesis and Characterization of Hybrid Gels. The ss-pLG was synthesized according to our earlier reported paper.[15] Gravimetric yield of the synthesized ss-pLG was estimated as 89.56%. Therefore, approximately 84.1% of gelatin was grafted into the backbone ss-PDLLA. Scheme 1 represents the synthesis of hybrid silica cross-linked gelatin grafted star-shaped PDLLA (h-ss-pLG) using GPTMS. The epoxy ring of the GPTMS molecules reacted with carboxyl groups on ss-pLG. This formed pendent silanol groups (Si−OH). Further, the condensation of two Si−OH molecules was held and formed Si−O−Si bonds. The chemistry for the synthesis of hybrid gelatin (h-Gel) was similar to that of h-ss-pLG.[22] The synthesized hybrid gels h-Gel and h-ss-pLG were characterized initially by using FTIR. Figure 1A, i and ii, shows the FTIR spectra of hybrid gels of h-Gel and h-ss-pLG, respectively. The unmodified Gel and ss-pLG polymer was also characterized to compare it with the synthesized silane cross-linked hybrid gels. We were able to observe the disappearance of Si−OH band at 910 cm^{-1} and appearance of broadened Si−O−Si band at 1115 cm^{-1} in the FT-IR spectrum of the hybrid gels; this suggested the formation of a highly condensed interpenetrating silica network (Figure 1A and Figure S1), We found the characteristic peaks for Gel and ss-pLG at 1661 and 1688 cm^{-1} representing its distinct C═O bond vibra-

DOI: 10.1021/acsabm.9b00680
ACS Appl. Bio Mater. 2020, 3, 197−207

tion.[15,25,34] After cross-linking of GPTMS with Gel and ss-pLG, the C═O stretching peaks shifted to lower frequencies at 1642 and 1627 cm^{-1}, which confirmed the strong covalent interaction between ss-pLG and GPTMS: Gel and GPTMS, respectively.

Further, we studied the thermal properties of the synthesized hybrid gel (Figure 1B,C). Figure 1B shows the thermogravimetric analysis (TGA) of unmodified and hybrid gel. Thermal degradation profile of unmodified and hybrid gels were quite different. The unmodified polymers Gel and ss-pLG showed its T_{onset} at 225 and 209 °C whereas T_{max} of the polymers were found as 457 and 455 °C, respectively (Table 1). Moreover,

Table 1. Thermal Degradation Properties of Gel, ss-pLG, and h-Gel, h-ss-pLG Determined by TGA

Sample no	Sample(s)	T_{onset}(°C)	T_{max}(°C)
1	Gel	225	457
2	ss-pLG	209	455
3	h-Gel	311	495
4	h-ss-pLG	326	504

the hybrid gels of h-Gel and h-ss-pLG showed improved thermal properties, where T_{max} for h-Gel and h-ss-pLG were found as 495 and 504 °C, respectively. The strong covalent binding of GPTMS with the respective polymer produced improved thermal properties in the case of hybrid gels.

DSC thermograms of Gel, ss-pLG, and modified h-Gel, h-s-pLG are shown in Figure 1C. T_g values of Gel, ss-pLG, h-Gel, and h-ss-pLG were observed at 142.9, 112.59, 114.87, and 126.46 °C, respectively. The shifting of T_g clearly indicates the successful cross-linking. On the other hand, T_g of h-Gel was reduced from its counterpart, Gel. The reduced T_g of h-Gel could be due to self-assembly of the molecules and condensation of a water molecule from them. The condensation will lead to reduction in the molecular weight.

3.2. Fabrication and Characterization of Scaffolds. The hybrid gels were frozen and freeze−dried to get porous scaffolds. It is to be noted that the structural complexity of tissue engineering scaffolds should be similar to native tissue in order to facilitate the required biological function.[35] Biological tissues generally have a gradient porous structure where porosity is not uniform. Rather, the natural engineering of porous architecture will be in such a way to maximize the overall performance of the structure. For instance, scaffolds employed in angiogenesis process (regeneration of a blood vessel/vascularization) should have the pores with a diameter of 20 to 40 μm for the exchange of metabolic components and to facilitate neovascularization.[36] Even though higher pore sizes and porosity may facilitate nutrient and oxygen delivery and enable more cell growth, the large amount of void volume may mitigate the mechanical properties of the scaffold.[37]

We used scanning electron microscopy (SEM) to gain qualitative surface morphology information about the molecular architecture of newly fabricated h-Gel and h-ss-pLG scaffolds. Figure 2 shows the SEM image of h-Gel and h-ss-pLG, respectively. h-Gel displayed a distorted elliptical porous architecture with pore sizes approximately ranging 35 ± 12 μm. However, it is to be noted that not all the pores were of uniform size—pore sizes were in the range from 20 to 50 μm. On the contrary, the resulting h-ss-pLG 3D scaffolds showed thicker walls of 3D morphology and pore sizes were 40 ± 8 μm.

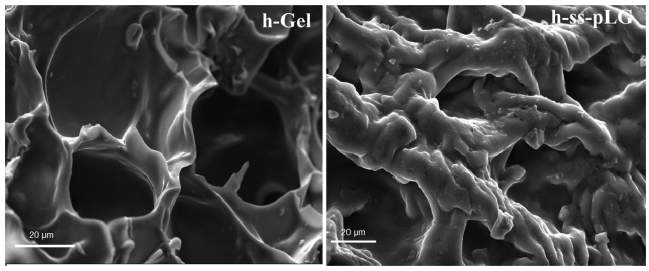

Figure 2. Surface morphology of hybrid scaffolds analyzed by SEM. The hybrid gels were freeze−dried and scaffolds were prepared.

3.3. Influence of Cross-Linking on Cell Proliferation within Hybrid Scaffolds. The surface hydrophobicity is a key factor which governs the cell response. Water contact angle was used to characterize the hydrophilicity of the newly synthesized h-Gel and h-ss-pLG. The contact angle measurement indicates that Gel and ss-pLG were more hydrophilic than the hybrid h-Gel and h-ss-pLG (Figure 3A). The higher hydrophobicity of h-ss-pLG than h-Gel could be attributed to the efficient cross-linking of GPTMS with ss-pLG and Gel.

We then examined the *in vitro* cell proliferation within the hybridized h-Gel and h-ss-pLG by studying the cell metabolic activity using 3-(4,5-dimethylthiazol-2-yl)-2,5-diphenyltetrazolium bromide) (MTT). The MTT absorbance values for h-Gel and h-ss-pLG were lower than those of the unmodified Gel and ss-pLG after 3 days of culturing (Figure 3B). This indicates a reduction in the rate of cell proliferation and reduction in overall cell viability. Furthermore, we performed MTT assay for various concentration of (0.1−2%) of GPTMS. Increasing the concentration of GPTMS induces cytotoxicity in a concentration-dependent manner until 1%, and there was no significant difference from 1−2% GPTMS, which was the additional component involved to make the hybrid gel (Figure 3C). We have already reported that ss-pLG is biocompatible and it supports cell proliferation.[15] Of note, 2% GPTMS showed less than 6% cytotoxicity, which is within the accepted range (10%). Therefore, it is clear that GPTMS plays a less significant role in inducing the cytotoxicity. MTT assay indicates a reduction in cell proliferation and cell viability that is independent of GPTMS concentration.

To understand the cell proliferation behavior at the molecular level, we studied the gene expression profiles of key genes that are involved in cell proliferation, invasion, and metastasis using quantitative polymerase chain reaction (qPCR) experiment. We studied the gene expression profile of *TWSIT, SOX2*, and *VEGF* that are associated with cell growth,[38] invasion,[39] and metastasis,[40] respectively. Figure 3D,E,F shows the molecular gene expression of cells grown in hybrid scaffolds. h-ss-pLG showed a 1.0-fold increase in *TWIST* mRNA expression after day 1 compared to h-Gel. The level of *TWIST* mRNA were reduced after Day 5 in both h-Gel and h-ss-pLG groups. The mRNA expression of *TWIST* in h-ss-pLG remained 0.5-fold greater than h-Gel after day 5. However, after day 7, *TWIST* expression was drastically reduced in h-ss-pLG (2.5 fold lower than h-Gel), indicating reduced cell proliferation in h-ss-pLG group. We observed a significant decrease in the gene expression of both *SOX2* and *VEGF* in cells cultured in h-ss-pLG compared to h-Gel scaffolds. The *TWIST* gene expression was higher in h-ss-pLG compared to h-Gel because of the degree of gelatin grafting in the PDLLA backbone. As evident from the SOX2 and VEGF

DOI: 10.1021/acsabm.9b00680
ACS Appl. Bio Mater. 2020, 3, 197−207

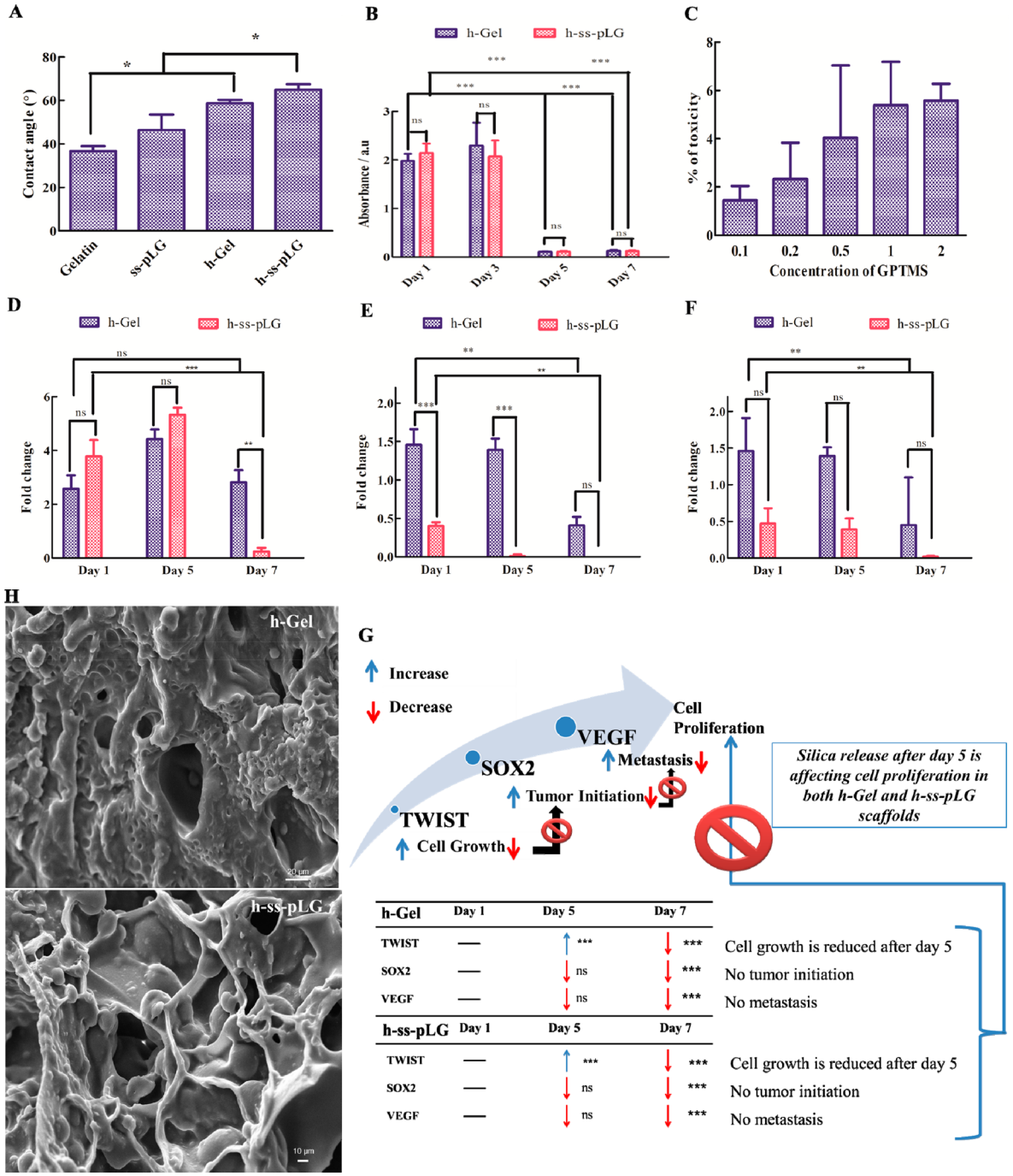

Figure 3. Demonstration of cell proliferation within the hybrid scaffolds and their molecular characterization. (A) Water contact angle measurements of polymer coated cover glass. (B) Rate of cell proliferation of Hep-G2 within the scaffolds assessed using MTT assay. (C) Cytotoxicity of GPTMS at various concentrations against Hep-G2. Molecular gene expression (D) TWIST, (E) SOX, and (F) VEGF of cells within hybrid scaffolds. (G) Schematic expression of silica release affecting the molecular expression of the proteins. (H) Surface morphology of cells seeded hybrid scaffolds after 3 days of culturing. All bars expressed as mean values ± SD (n = 3) In the case of qPCR data, confidence intervals (CI) were taken and plotted as a graph instead of SD; * $p < 0.05$, **$p < 0.001$, *** $p < 0.0001$.

expression, the metastasis process had not proceeded, which could be because of the decrease in the rate of cell proliferation. Metastasis initiation (SOX2 expression) and propagation (VEGF expression) are both dependent on the expression of TWIST. Initially, until day 5 the TWIST expression was normal; however, after day 5, we observed a reduced TWIST expression. Further, we physically observed that the cells were being detached from the scaffold; therefore, it could be the reason for the reduced molecular expression levels of TWIST, which further leads to a decrease in the SOX2 expression and subsequently to reduced VEGF expression. Overall, we observed that the initiation and propagation of metastasis were arrested in the cell grown in h-ss-pLG scaffolds (Figure 3G).

Further, SEM images of Hep-G2 cell-seeded scaffolds were acquired to check the cellular growth behavior within 3D scaffolds. We observed that the thick wall of h-ss-pLG became thinner and better cell growth appeared in h-ss-pLG compared

DOI: 10.1021/acsabm.9b00680
ACS Appl. Bio Mater. 2020, 3, 197−207

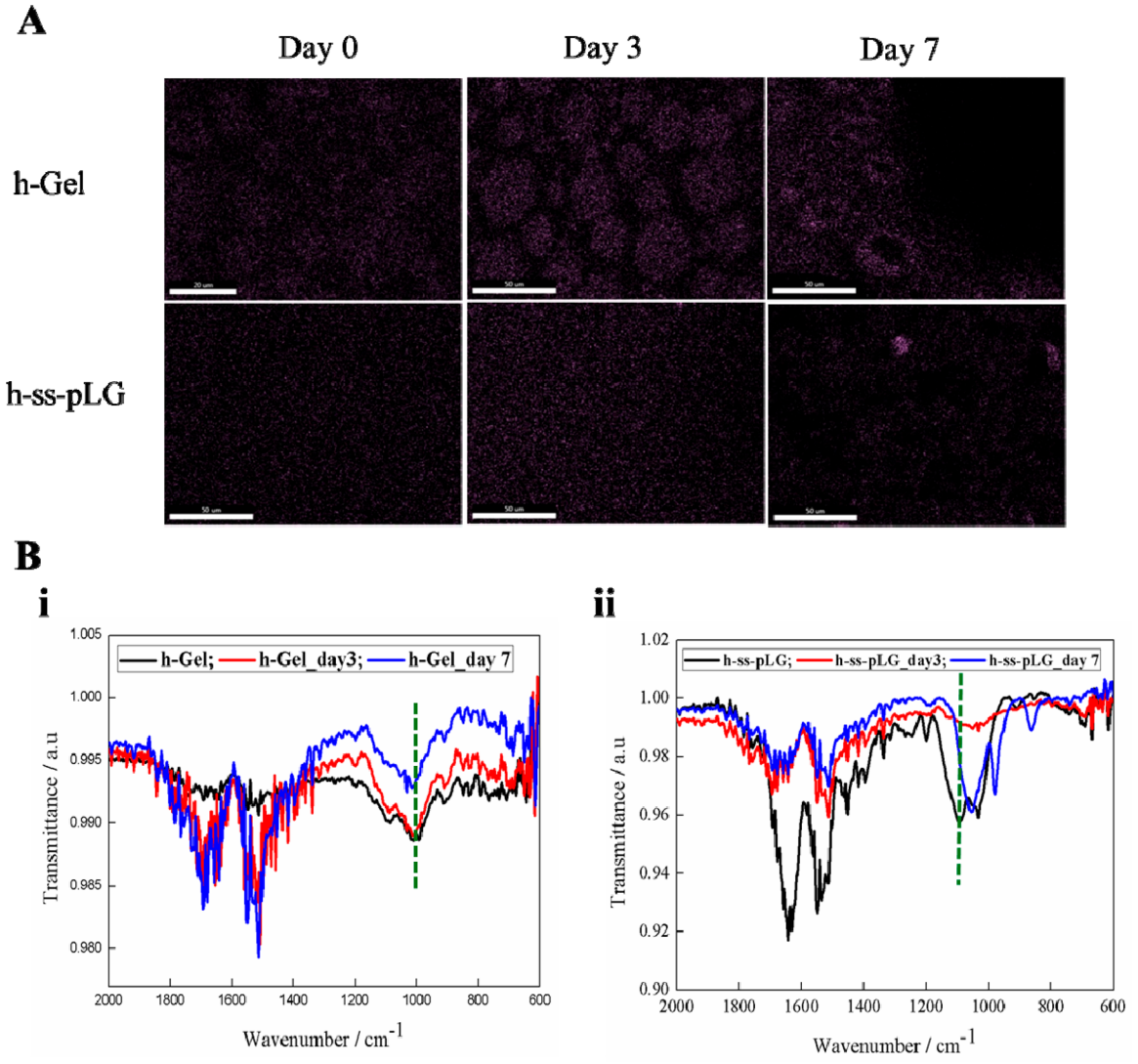

Figure 4. Qualitative release kinetics of silica from hybrid scaffolds. (A) Elemental mapping and (B) FTIR of hybrid scaffolds before and after incubating in cell culture media.

to h-Gel (Figure 3H). We were not able to track any cells after 7 days of culturing through SEM.

3.4. Silica Release May Affect Cell Proliferation. We observed a decrease in the rate of cell proliferation in silane cross-linked hybrid scaffolds (h-Gel and h-ss-pLG). However, the reason for the reduction in cellular proliferation stands unaddressed owing to a less significant effect of GPTMS on cytotoxicity against Hep-G2 cells. To identify the reason, we framed a hypothesis that silica release from the silane cross-linked h-ss-pLG affects the rate of HepG2 cell proliferation. We had a strong rationale to support our hypothesis, because previous reports indicate that silica material possess good cell adhesion property.[18,41] We believed that the release of silica might trigger the detachment of cells that are attached to silica. In order to validate our hypothesis, we quantified the initial silica level (%silica) present in the hybrid scaffold. We assessed the silica level after day 3 and day 7 (post cell culture media incubation) by energy-dispersive X-ray analyzer (EDX). Interestingly we observed the reduction in the silica profile of the scaffold.

Figure 4A shows the silica release profile at day 0, 3, and 7 observed by elemental mapping through EDX for the h-Gel and h-ss-pLG samples. We observed the decrease in the intensity of silica element after day 3 and 7 of incubation in the cell culture media. The silica quantity (%silica) in h-Gel at Day 3 (20.58 ± 3.27) was lower than the initial silica level at day 0 (22.81 ± 3.11); this was further reduced to 15.95 ± 3.37 on day 7. Similarly, the %silica in h-ss-pLG at day 7 (14.83 ± 3.72) was much lower than the %silica at day 0 (18.27 ± 5.94) and day 3 (15.3 ± 3.84) (Table 2). The significant level of silica released from the scaffold to cell culture medium observed by EDX provides strong evidence to validate our hypothesis. Furthermore, we studied the silica release profile in h-Gel and h-ss-pLG by FTIR after day 3 and day 7. We observed the Si−O−Si in the phase stretching band around

Table 2. Quantitative Release Kinetics of Silica from Hybrid Scaffolds Assessed by EDX Analysis

		after incubation in cell culture media	
sample	Day 0	Day 3	Day 7
h-Gel	22.81 ± 3.11	20.58 ± 3.27	15.95 ± 3.37
h-ss-pLG	18.27 ± 5.94	15.3 ± 3.84	14.83 ± 3.72

DOI: 10.1021/acsabm.9b00680
ACS Appl. Bio Mater. 2020, 3, 197−207

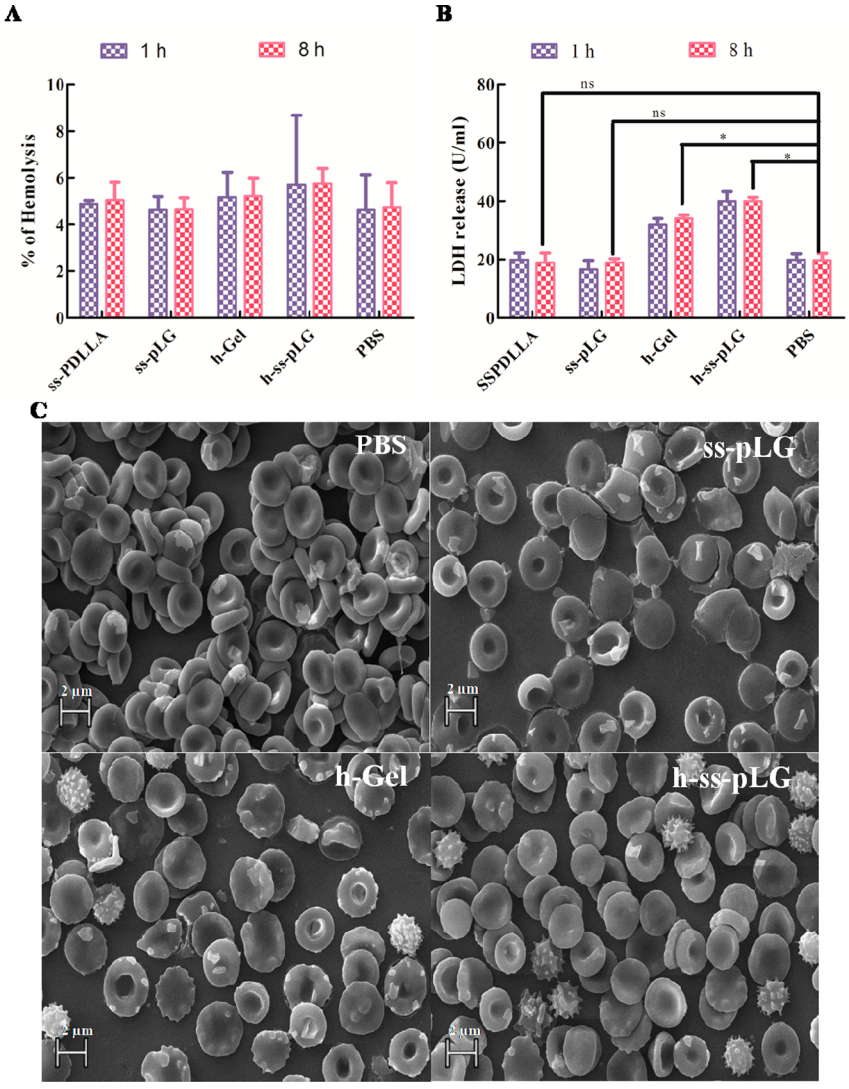

Figure 5. Hemocompatibility of hybrid scaffolds compared to its counterpart. (A) Hemolysis of the scaffolds after 1 and 8 h; no significant differences were observed compared to PBS (negative control). (B) Erythrocyte membrane integrity using LDH release assay. (C) Morphology of RBCs after 4 h incubation with hybrid scaffolds. Scale bar 2 μm.

1115 cm^{-1}. The decrease in the Si−O−Si band stretching indicates the release of silica with time (Figure 4B). The wide FTIR spectrum is given in Figure S2. The dissolution property of silica from chitosan-based hybrid scaffolds had also been reported, which complies with our observation.[25]

In addition, we further cultured L929 cells on hybrid polymers (h-Gel and h-ss-pLG) and un-cross-linked polymers (Gel and ss-pLG) coated 2D cover glass and stained with Rhodamine phalloidin to evaluate the morphology of fibroblasts. We observed that the cells came out of the plane and there was a significant change in the morphology of polymers which could be attributed to the release of silane (Figure S3). Therefore, it could be attributed to the silica release affecting the cellular proliferation as silica inherently had the cell adhesion property.

3.5. Influence of Silane Cross-Linking on Hemocompatibility. We next studied the hemocompatibility of the h-Gel and h-ss-pLG in human blood, *in vitro*. Normally, platelets do not adhere to endothelial cells in the circulating blood. However, when blood is exposed to a foreign surface the platelets tend to deposit and form a layer of proteins and cells, is followed by immune system activation and initiation of the coagulation process. The hemolysis was studied *in vitro*. The hemolysis was found to be <6% for all the scaffolds evaluated. The h-Gel and h-ss-pLG scaffolds showed no significant difference when compared to their respective unmodified counterparts after 1 and 8 h (Figure 5A). Further, the hemolysis was high for h-Gel and h-ss-pLG, at both 1 h and 8 h. However, hemolysis ≤10% has been considered as hemocompatible.[42]

Similarly, the membrane integrity of erythrocytes was evaluated by quantifying the enzyme LDH, when they were incubated with scaffolds. After 1 and 8 h intervals, the ss-PDLLA and ss-pLG incubated with erythrocytes did not show any significant increase, whereas a significant increase in the release of LDH was observed for hybrid scaffolds (h-Gel and h-ss-pLG) ($p > 0.05$) when compared to PBS (negative control). This could be attributed to the hydrophobicity of hybrid scaffolds (Figure 5B). These results indicate that the hybrid scaffolds induce a small disturbance in the membrane integrity of erythrocytes.

DOI: 10.1021/acsabm.9b00680
ACS Appl. Bio Mater. 2020, 3, 197−207

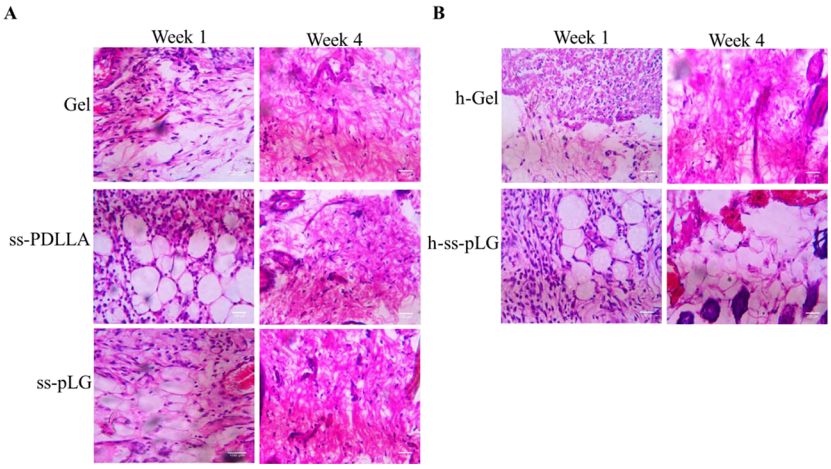

Figure 6. *In vivo* compatibility of hybrid scaffolds. H&E staining of retrieved acellular (A) unmodified and (B) hybrid scaffolds after 1 and 4 weeks of subcutaneous implantation in female rat.

Figure 5C presents the photomicrograph of SEM image displaying a negligible number of damaged RBCs when incubated with both h-Gel and h-ss-pLG. The qualitative imaging results comply with our quantitative hemolysis and LDH release. Thus, the silane cross-linking has a less significant effect on the hemcompatibility.

3.6. Influence of Silane Cross-Linking on Immune Response *in Vivo*. *In vivo* experiments were conducted to evaluate the host immune response and implant integration of the scaffolds. We investigated the biodegradation and tissue biocompatibility of unmodified and hybrid acellular scaffolds after subcutaneous implantation in rat; after 1 and 4 weeks post implantation, we retrieved the scaffolds from the implanted site with the overlying native tissues and performed histological examination to assess the infiltration of inflammatory cells. The incision led to a loss in the weight of the animals and animals were gaining weight slowly. The rate of weight gain was relatively good compared to the Sham group (Table S2). Figure S4 presents the photomicrographs of the animals at the implant site after 4 weeks of study.

Figure 6 shows the H&E stain of the subcutaneous tissue after the implantation of scaffolds. Higher cell infiltration and cell attachment were observed after week 1 in all the tested scaffolds. The unmodified Gel, ss-PDLLA, and ss-pLG scaffolds were completely degraded after week 4; the excised tissue was morphologically similar to the control tissue, which indicates the degraded product or the scaffold did not affect the host tissue. On the other hand, the hybrid scaffolds h-Gel and h-ss-pLG were not degraded completely as the Gel, ss-PDLLA, and ss-pLG. This could be attributed to silane cross-linking which increased the stability of hybrid scaffolds. Further, there were no significant changes observed in infiltration of cells for h-Gel and h-ss-pLG scaffolds compared to Gel, ss-PDLLA, and ss-pLG. The results from the animal study demonstrated that hybrid scaffolds have good tissue compatibility; at the same time, they were not degraded completely within 4 weeks of the study because of silane cross-linking.

There have been a number of biodegradable polymers using cross-linkers widely explored as scaffold systems for tissue engineering applications. The degradation of collagen (the natural omnipresent structural protein present in the body) was affected by the cross-linking and ranging from 1 to 4 weeks or longer *in vivo*.[43] The silk fibronin, another natural protein, showed various degradation times from 2 months to 1 year based on the processing of the scaffold.[44] The degradation of synthetic biodegradable polymers PCL and PLGA was found as 2 years[45] and 26 weeks,[46,47] respectively. The long-term biodegradable scaffolds because of cross-linking or by its inherent nature could be used for soft tissue engineering applications such as ligament repair, cartilage regeneration,[48] pediatric cardiovascular surgery involving biocompatible materials,[49,50] and bone implant application.[51] Also, long-term biodegradable scaffolds can be used for local delivery of drugs.[52]

4. CONCLUSION

To conclude, our findings indicate an increase in the hydrophobicity and stability of the hybrid scaffolds (h-ss-pLG and h-Gel) when they were cross-linked with GPTMS. However, our *in vitro* results indicate a decrease in the rate of cell proliferation within the silane cross-linked hybrid scaffolds (h-Gel and h-ss-pLG) after day 3. We arrived to the conclusion based on the observation that GPTMS *per se* at concentrations used have not shown any significant cytotoxicity, and the reduction in the rate of cell proliferation was highly aligned with the release of silica that was confirmed by FT-IR and EDX elemental mapping experiments. We postulate that cells adhered on the silica matrix may become detached while the silica is released from the hybrid scaffold that could directly influence a decrease in the rate of cell proliferation within the scaffold. Concurrently, the *in vivo* subcutaneous implantation study showed that Gel, ss-PDLLA, and ss-pLG scaffolds degraded completely after week 4, whereas the hybrid scaffolds h-ss-pLG and h-Gel were not degraded, which could also be due to the silane cross-linking. We anticipate our results to open up new avenues in the cross-linker selection while facilitating the stability of the tissue culture scaffold without affecting their biological functions. Therefore, it is critical to understand the biological behavior of the scaffold and its components including the cross-linkers prior to its specific use.

■ ASSOCIATED CONTENT

Supporting Information

The Supporting Information is available free of charge at https://pubs.acs.org/doi/10.1021/acsabm.9b00680.

DOI: 10.1021/acsabm.9b00680
ACS Appl. Bio Mater. 2020, 3, 197−207

Synthesis procedures and characterization of polymers (PDF)

AUTHOR INFORMATION

Corresponding Author

*E-mail: nmishra.bme@iitbhu.ac.in.

ORCID

Chelladurai Karthikeyan Balavigneswaran: 0000-0002-9715-0034

Prakash Shyam Karuppiah: 0000-0003-0062-4537

Nira Misra: 0000-0002-6884-8951

Notes

The authors declare no competing financial interest.

ACKNOWLEDGMENTS

Authors would like to acknowledge Central Instrumentation Facility Centre (CIFC), IIT(BHU) for the characterization of polymers using FTIR and SEM. Authors extend their acknowledgment of the financial support from Ministry of human resource and development (MHRD), India in terms of fellowship.

REFERENCES

(1) Jones, J. R. Reprint of: Review of bioactive glass: From Hench to hybrids. *Acta Biomater.* **2015**, *23*, S53−S82.

(2) Wei, G.; Ma, P. X. Structure and properties of nano-hydroxyapatite/polymer composite scaffolds for bone tissue engineering. *Biomaterials* **2004**, *25* (19), 4749−4757.

(3) Rezwan, K.; Chen, Q.; Blaker, J.; Boccaccini, A. R. Biodegradable and bioactive porous polymer/inorganic composite scaffolds for bone tissue engineering. *Biomaterials* **2006**, *27* (18), 3413−3431.

(4) Abou Neel, E. A.; Pickup, D. M.; Valappil, S. P.; Newport, R. J.; Knowles, J. C. Bioactive functional materials: a perspective on phosphate-based glasses. *J. Mater. Chem.* **2009**, *19* (6), 690−701.

(5) Bigi, A.; Cojazzi, G.; Panzavolta, S.; Rubini, K.; Roveri, N. Mechanical and thermal properties of gelatin films at different degrees of glutaraldehyde crosslinking. *Biomaterials* **2001**, *22* (8), 763−768.

(6) Matsuda, S.; Iwata, H.; Se, N.; Ikada, Y. Bioadhesion of gelatin films crosslinked with glutaraldehyde. *J. Biomed. Mater. Res.* **1999**, *45* (1), 20−27.

(7) Lai, J.-Y.; Li, Y.-T. Evaluation of cross-linked gelatin membranes as delivery carriers for retinal sheets. *Mater. Sci. Eng., C* **2010**, *30* (5), 677−685.

(8) Lai, J.-Y.; Luo, L.-J.; Ma, D. Effect of Cross-Linking Density on the Structures and Properties of Carbodiimide-Treated Gelatin Matrices as Limbal Stem Cell Niches. *Int. J. Mol. Sci.* **2018**, *19* (11), 3294.

(9) Bigi, A.; Cojazzi, G.; Panzavolta, S.; Roveri, N.; Rubini, K. Stabilization of gelatin films by crosslinking with genipin. *Biomaterials* **2002**, *23* (24), 4827−4832.

(10) Novak, B. M. Hybrid nanocomposite materials—between inorganic glasses and organic polymers. *Adv. Mater.* **1993**, *5* (6), 422−433.

(11) Wang, D.; Romer, F.; Connell, L.; Walter, C.; Saiz, E.; Yue, S.; Lee, P. D.; McPhail, D. S.; Hanna, J. V.; Jones, J. R. Highly flexible silica/chitosan hybrid scaffolds with oriented pores for tissue regeneration. *J. Mater. Chem. B* **2015**, *3* (38), 7560−7576.

(12) Wang, Y.; Wang, X.; Xiang, Y.; Zhang, Z.; Liu, M.; Wei, Q.; Jiang, X.; Ma, C.; Ye, T.; Cui, W. Hydroxyapatite-Nanowires Enhanced Electrospun Fiber via Craze Disperse Stress for Bone Regeneration. *Nanosci. Nanotechnol. Lett.* **2018**, *10* (11), 1498−1507.

(13) Wang, Y.; Yan, L.; Cheng, R.; Muhtar, M.; Shan, X.; Xiang, Y.; Cui, W. Multifunctional HA/Cu nano-coatings on titanium using PPy coordination and doping via pulse electrochemical polymerization. *Biomater. Sci.* **2018**, *6* (3), 575−585.

(14) Xin, T.; Gu, Y.; Cheng, R.; Tang, J.; Sun, Z.; Cui, W.; Chen, L. Inorganic strengthened hydrogel membrane as regenerative periosteum. *ACS Appl. Mater. Interfaces* **2017**, *9* (47), 41168−41180.

(15) Balavigneswaran, C. K.; Mahto, S. K.; Subia, B.; Prabhakar, A.; Mitra, K.; Rao, V.; Ganguli, M.; Ray, B.; Maiti, P.; Misra, N. Tailored chemical properties of 4-arm star shaped poly (D, L-lactide) as cell adhesive three-dimensional scaffolds. *Bioconjugate Chem.* **2017**, *28* (4), 1236−1250.

(16) Balavigneswaran, C. K.; Mahto, S. K.; Mahanta, A. K.; Singh, R.; Vijayakumar, M. R.; Ray, B.; Misra, N. Cell proliferation influenced by matrix compliance of gelatin grafted poly (d, l-Lactide) three dimensional scaffolds. *Colloids Surf., B* **2018**, *166*, 170−178.

(17) Periasamy, V. S.; Athinarayanan, J.; Alshatwi, A. A. Extraction and biocompatibility analysis of silica phytoliths from sorghum husk for three-dimensional cell culture. *Process Biochem.* **2018**, *70*, 153−159.

(18) Lord, M.; Cousins, B.; Doherty, P.; Whitelock, J.; Simmons, A.; Williams, R.; Milthorpe, B. The effect of silica nanoparticulate coatings on serum protein adsorption and cellular response. *Biomaterials* **2006**, *27* (28), 4856−4862.

(19) Shadjou, N.; Hasanzadeh, M. Bone tissue engineering using silica-based mesoporous nanobiomaterials: Recent progress. *Mater. Sci. Eng., C* **2015**, *55*, 401−409.

(20) Tonda-Turo, C.; Gentile, P.; Saracino, S.; Chiono, V.; Nandagiri, V.; Muzio, G.; Canuto, R. A.; Ciardelli, G. Comparative analysis of gelatin scaffolds crosslinked by genipin and silane coupling agent. *Int. J. Biol. Macromol.* **2011**, *49* (4), 700−706.

(21) Tonda-Turo, C.; Cipriani, E.; Gnavi, S.; Chiono, V.; Mattu, C.; Gentile, P.; Perroteau, I.; Zanetti, M.; Ciardelli, G. Crosslinked gelatin nanofibres: Preparation, characterisation and in vitro studies using glial-like cells. *Mater. Sci. Eng., C* **2013**, *33* (5), 2723−2735.

(22) Mahony, O.; Tsigkou, O.; Ionescu, C.; Minelli, C.; Ling, L.; Hanly, R.; Smith, M. E.; Stevens, M. M.; Jones, J. R. Silica-gelatin hybrids with tailorable degradation and mechanical properties for tissue regeneration. *Adv. Funct. Mater.* **2010**, *20* (22), 3835−3845.

(23) Yoon, B.-H.; Kim, H.-E.; Kim, H.-W. Bioactive microspheres produced from gelatin−siloxane hybrids for bone regeneration. *J. Mater. Sci.: Mater. Med.* **2008**, *19* (6), 2287−2292.

(24) Liu, Y.-L.; Su, Y.-H.; Lai, J.-Y. In situ crosslinking of chitosan and formation of chitosan−silica hybrid membranes with using γ-glycidoxypropyltrimethoxysilane as a crosslinking agent. *Polymer* **2004**, *45* (20), 6831−6837.

(25) Connell, L. S.; Romer, F.; Suárez, M.; Valliant, E. M.; Zhang, Z.; Lee, P. D.; Smith, M. E.; Hanna, J. V.; Jones, J. R. Chemical characterisation and fabrication of chitosan−silica hybrid scaffolds with 3-glycidoxypropyl trimethoxysilane. *J. Mater. Chem. B* **2014**, *2* (6), 668−680.

(26) Miyama, M.; Yang, Y.; Yasuda, T.; Okuno, T.; Yasuda, H. K. Static and dynamic contact angles of water on polymeric surfaces. *Langmuir* **1997**, *13* (20), 5494−5503.

(27) Guan, J.; Fujimoto, K. L.; Sacks, M. S.; Wagner, W. R. Preparation and characterization of highly porous, biodegradable polyurethane scaffolds for soft tissue applications. *Biomaterials* **2005**, *26* (18), 3961−3971.

(28) Frydrych, M.; Román, S.; MacNeil, S.; Chen, B. Biomimetic poly (glycerol sebacate)/poly (l-lactic acid) blend scaffolds for adipose tissue engineering. *Acta Biomater.* **2015**, *18*, 40−49.

(29) Balachander, G. M.; Balaji, S. A.; Rangarajan, A.; Chatterjee, K. Enhanced metastatic potential in a 3D tissue scaffold toward a comprehensive in vitro model for breast cancer metastasis. *ACS Appl. Mater. Interfaces* **2015**, *7* (50), 27810−27822.

(30) Rao, X.; Huang, X.; Zhou, Z.; Lin, X. An improvement of the 2^(−delta delta CT) method for quantitative real-time polymerase chain reaction data analysis. *Biostatistics, bioinformatics and biomathematics* **2013**, *3* (3), 71.

(31) Vijayakumar, M. R.; Vajanthri, K. Y.; Balavigneswaran, C. K.; Mahto, S. K.; Mishra, N.; Muthu, M. S.; Singh, S. Pharmacokinetics, biodistribution, in vitro cytotoxicity and biocompatibility of Vitamin E

DOI: 10.1021/acsabm.9b00680
ACS Appl. Bio Mater. 2020, 3, 197−207

TPGS coated trans resveratrol liposomes. *Colloids Surf., B* **2016**, *145*, 479−491.
(32) Bender, E. A.; Adorne, M. D.; Colomé, L. M.; Abdalla, D. S.; Guterres, S. S.; Pohlmann, A. R. Hemocompatibility of poly (ε-caprolactone) lipid-core nanocapsules stabilized with polysorbate 80-lecithin and uncoated or coated with chitosan. *Int. J. Pharm.* **2012**, *426* (1), 271−279.
(33) Kumar, M.; Nandi, S. K.; Kaplan, D. L.; Mandal, B. B. Localized immunomodulatory silk macrocapsules for islet-like spheroid formation and sustained insulin production. *ACS Biomater. Sci. Eng.* **2017**, *3* (10), 2443−2456.
(34) Ghasemi-Mobarakeh, L.; Prabhakaran, M. P.; Morshed, M.; Nasr-Esfahani, M.-H.; Ramakrishna, S. Electrospun poly (ε-caprolactone)/gelatin nanofibrous scaffolds for nerve tissue engineering. *Biomaterials* **2008**, *29* (34), 4532−4539.
(35) Smidsrod, O. Molecular basis for some physical properties of alginates in the gel state. *Faraday Discuss. Chem. Soc.* **1974**, *57* (0), 263−274.
(36) Madden, L. R.; Mortisen, D. J.; Sussman, E. M.; Dupras, S. K.; Fugate, J. A.; Cuy, J. L.; Hauch, K. D.; Laflamme, M. A.; Murry, C. E.; Ratner, B. D. Proangiogenic scaffolds as functional templates for cardiac tissue engineering. *Proc. Natl. Acad. Sci. U. S. A.* **2010**, *107* (34), 15211−6.
(37) Karageorgiou, V.; Kaplan, D. Porosity of 3D biomaterial scaffolds and osteogenesis. *Biomaterials* **2005**, *26* (27), 5474−91.
(38) Shiota, M.; Izumi, H.; Onitsuka, T.; Miyamoto, N.; Kashiwagi, E.; Kidani, A.; Yokomizo, A.; Naito, S.; Kohno, K. Twist promotes tumor cell growth through YB-1 expression. *Cancer Res.* **2008**, *68* (1), 98−105.
(39) Sun, C.; Sun, L.; Li, Y.; Kang, X.; Zhang, S.; Liu, Y. Sox2 expression predicts poor survival of hepatocellular carcinoma patients and it promotes liver cancer cell invasion by activating Slug. *Med. Oncol.* **2013**, *30* (2), 503.
(40) Fischbach, C.; Chen, R.; Matsumoto, T.; Schmelzle, T.; Brugge, J. S.; Polverini, P. J.; Mooney, D. J. Engineering tumors with 3D scaffolds. *Nat. Methods* **2007**, *4* (10), 855.
(41) Lopez-Alvarez, M.; Solla, E.; González, P.; Serra, J.; Leon, B.; Marques, A.; Reis, R. Silicon−hydroxyapatite bioactive coatings (Si−HA) from diatomaceous earth and silica. Study of adhesion and proliferation of osteoblast-like cells. *J. Mater. Sci.: Mater. Med.* **2009**, *20* (5), 1131−1136.
(42) Amin, K.; Dannenfelser, R. M. In vitro hemolysis: guidance for the pharmaceutical scientist. *J. Pharm. Sci.* **2006**, *95* (6), 1173−1176.
(43) Ueda, H.; Hong, L.; Yamamoto, M.; Shigeno, K.; Inoue, M.; Toba, T.; Yoshitani, M.; Nakamura, T.; Tabata, Y.; Shimizu, Y. Use of collagen sponge incorporating transforming growth factor-β1 to promote bone repair in skull defects in rabbits. *Biomaterials* **2002**, *23* (4), 1003−1010.
(44) Wang, Y.; Rudym, D. D.; Walsh, A.; Abrahamsen, L.; Kim, H.-J.; Kim, H. S.; Kirker-Head, C.; Kaplan, D. L. In vivo degradation of three-dimensional silk fibroin scaffolds. *Biomaterials* **2008**, *29* (24−25), 3415−3428.
(45) Sun, H.; Mei, L.; Song, C.; Cui, X.; Wang, P. The in vivo degradation, absorption and excretion of PCL-based implant. *Biomaterials* **2006**, *27* (9), 1735−1740.
(46) Liao, S.; Watari, F.; Zhu, Y.; Uo, M.; Akasaka, T.; Wang, W.; Xu, G.; Cui, F. The degradation of the three layered nano-carbonated hydroxyapatite/collagen/PLGA composite membrane in vitro. *Dent. Mater.* **2007**, *23* (9), 1120−1128.
(47) Ramchandani, M.; Pankaskie, M.; Robinson, D. The influence of manufacturing procedure on the degradation of poly (lactide-co-glycolide) 85:15 and 50:50 implants. *J. Controlled Release* **1997**, *43* (2−3), 161−173.
(48) Pei, B.; Wang, W.; Fan, Y.; Wang, X.; Watari, F.; Li, X. Fiber-reinforced scaffolds in soft tissue engineering. *Regenerative biomaterials* **2017**, *4* (4), 257−268.
(49) Matsumura, G.; Nitta, N.; Matsuda, S.; Sakamoto, Y.; Isayama, N.; Yamazaki, K.; Ikada, Y. Long-term results of cell-free biodegradable scaffolds for in situ tissue-engineering vasculature: in a canine inferior vena cava model. *PLoS One* **2012**, *7* (4), No. e35760.
(50) Matsumura, G.; Isayama, N.; Matsuda, S.; Taki, K.; Sakamoto, Y.; Ikada, Y.; Yamazaki, K. Long-term results of cell-free biodegradable scaffolds for in situ tissue engineering of pulmonary artery in a canine model. *Biomaterials* **2013**, *34* (27), 6422−6428.
(51) Shkarina, S.; Shkarin, R.; Weinhardt, V.; Melnik, E.; Vacun, G.; Kluger, P. J.; Loza, K.; Epple, M.; Ivlev, S. I.; Baumbach, T. 3D biodegradable scaffolds of polycaprolactone with silicate-containing hydroxyapatite microparticles for bone tissue engineering: High-resolution tomography and in vitro study. *Sci. Rep.* **2018**, *8* (1), 8907.
(52) Khang, G.; Rhee, J. M.; Jeong, J. K.; Lee, J. S.; Kim, M. S.; Cho, S. H.; Lee, H. B. Local drug delivery system using biodegradable polymers. *Macromol. Res.* **2003**, *11* (4), 207−223.

DOI: 10.1021/acsabm.9b00680
ACS Appl. Bio Mater. 2020, 3, 197−207